EARTHQUAKE ENGINEERING AND STRUCTURAL DYNAMICS, VOL. 25, 795-814 (1996)

INFLUENCE OF SEISMIC WAVES SPATIAL VARIABILITY ON BRIDGES: A SENSITIVITY ANALYSIS

MICHEL KAHAN

Laboratoire des Matériaux et des Structures du Génie Civil, LCPC-CNRS UMR113, 2 alleé Képler, 77240 Champs sur Marne, France

RENÉ-JEAN GIBERT

Centre d'Etudes de Mecanique d'Ile de France, Université d'Evry Val d'Essonne, France

AND

PIERRE-YVES BARD

Laboratoire de Géophysique Interne et Tectonophysique, Observatoire de Grenoble, France

SUMMARY

The sensitivity of bridges to spatial variations of seismic ground motions is studied within the framework of the multiple support response spectrum (MSRS) method developed by Der Kiureghian and Neuenhofer (*Earthquake eng. struct. dyn.* **21**, 713–740 (1992)). A simplified approximate formula for small spatial variations of seismic motions sheds some light on the response of bridges: the pseudo-static contribution which is commonly introduced to account for static effects of relative ground displacements may be neglected in case of lateral or vertical ground displacements but may contribute significantly to the response in case of longitudinal ground motions. Mode shapes affect the dynamic contribution in the following way: spatial variability of ground motion increases the response of antisymmetrical modes and decreases that of swaying modes which lie on one side of the structure position at rest. The approximate formula indicates properly the trend of the response given by the MSRS rule for small ground motion spatial variability and may therefore be useful at a design stage. A criterion is given to estimate the number of modes that need to be included in the analysis. For large and/or uncertain spatial variability, an efficient algorithm based on the MSRS rule is proposed to obtain the maximum (conservative) response.

KEY WORDS: seismic waves spatial variability; bridges; multiple support response spectrum

INTRODUCTION

The seismic response of extended structures, such as bridges, subjected to non-uniform ground motion has widely become a concern to engineers and researchers alike. A better description of soil motions and the development of numerical methods that take into account the spatial variability of seismic movements are two factors that have enabled scientists to explore this aspect of earthquake engineering. Indeed, the nature and importance of the phenomena behind the spatial variability of seismic waves, namely the loss of coherency and the wave passage effect, are now better understood thanks to empirical studies based on recordings of strong motion arrays (essentially the SMART-1 array[2] in Lotung, Taiwan). In the wake of these studies, several stochastic models were elaborated and fitted to experimental data (e.g. see References 3–6). More recently, Der Kiureghian[7] has developed a theoretical model for the coherency function describing the spatial variability of earthquake ground motions, based on basic principles of random processes and some simplifying assumptions regarding the propagation of seismic waves.

The response and sensitivity of increasingly complex structures to these partially correlated ground motions has been studied in recent years. It turns out that for mechanically determinate structures, such as simply

CCC 0098-8847/96/080795-20

Received 16 February 1995
Revised 30 January 1996

supported beams excited transversely, the internal forces are reduced by the spatial variation of seismic motions.[8,9] The situation may be quite different for statically indeterminate structures such as portal frames[10,11] or arches[12] and indeterminate multi-span beams.[13–16] In fact, to properly describe the response of these structures, it is necessary to include pseudo-static terms that cover the static effect on the structure of differential ground motions. These terms generate internal forces and differential motions in indeterminate structures (particularly in rigid ones), whereas they do not in statically determinate structures. The effect of spatial variations of seismic motions is thus the result of a trade-off between an increase in the response due to pseudo-static terms and a decrease due to dynamic terms.

Suspension bridges[17–20] and cable-stayed bridges[21] show a complex sensitivity to spatial variations of ground motions partly because of the coupling between longitudinal and vertical motions and also because the cables increase the degree of static indetermination. It appears also that a greater number of modes may be necessary to properly describe the structural response when spatial variability of ground motions is introduced.

The general framework to study the influence of spatial variability on extended structures has been elaborated recently in the form of combination rules.[22–24,1,9] The multiple-support response spectrum (MSRS) rule[1] is briefly reviewed in this paper. The sensitivity of extended structures to small spatial variations of seismic motions is then analytically derived as a Taylor expansion of the maximum response given by the MSRS rule. The second order of the expansion sheds some light on the contribution of the pseudo-static and dynamic terms. A criterion to assess the number of modes that are needed is also given. It turns out, however, that the approximate formula based on the Taylor expansion fails to yield accurate results for large spatial variations of seismic motions or for structures with closely spaced eigenfrequencies. Also, the parameters of the variability models may not be given accurately, but only within a certain range of values. An optimization scheme is then proposed to find the maximum response over that domain.

SPECTRAL ANALYSIS FOR MULTIPLY SUPPORTED STRUCTURES

For the sake of simplicity, it is assumed that structures behave in a linear elastic fashion and that the free field soil motion is imposed on their supports (soil-structure interaction is thus disregarded). Although curved bridges fit very well in the analysis, only in-plane structures are considered herein. For a finite element model of the bridge, define $\mathbf{Y}$ [resp. $\mathbf{Z}$] the vector of the N [resp. NS] degrees of freedom of the structure [resp. of the foundations]. The equation of motion is as follows:[25]

$$\begin{bmatrix} \mathbf{M}_{\mathrm{s}} & \mathbf{M}_{\mathrm{sf}} \\ \mathbf{M}_{\mathrm{sf}}^{\mathrm{T}} & \mathbf{M}_{\mathrm{f}} \end{bmatrix} \begin{Bmatrix} \ddot{\mathbf{Y}} \\ \ddot{\mathbf{Z}} \end{Bmatrix} + \begin{bmatrix} \mathbf{C}_{\mathrm{s}} & \mathbf{C}_{\mathrm{sf}} \\ \mathbf{C}_{\mathrm{sf}}^{\mathrm{T}} & \mathbf{C}_{\mathrm{f}} \end{bmatrix} \begin{Bmatrix} \dot{\mathbf{Y}} \\ \dot{\mathbf{Z}} \end{Bmatrix} + \begin{bmatrix} \mathbf{K}_{\mathrm{s}} & \mathbf{K}_{\mathrm{sf}} \\ \mathbf{K}_{\mathrm{sf}}^{\mathrm{T}} & \mathbf{K}_{\mathrm{f}} \end{bmatrix} \begin{Bmatrix} \mathbf{Y} \\ \mathbf{Z} \end{Bmatrix} = \begin{Bmatrix} \mathbf{0} \\ \mathbf{F} \end{Bmatrix} \tag{1}$$

in which $\mathbf{M}$, $\mathbf{C}$, and $\mathbf{K}$ are mass, damping, and stiffness matrices, respectively. The subscripts s, f and sf are attached to the structure, foundations, and coupling terms. The superstructure motion $\mathbf{Y}$ is the sum of a pseudo-static term $\mathbf{S}$ and a dynamic term $\mathbf{X}$:

$$\mathbf{Y} = \mathbf{S} + \mathbf{X}, \qquad \mathbf{S} = -\mathbf{K}_{\mathrm{s}}^{-1}\mathbf{K}_{\mathrm{sf}}\,\mathbf{Z} = \tilde{\mathbf{R}}\,\mathbf{Z} \tag{2}$$

where $\tilde{\mathbf{R}}$ is the influence matrix whose kth column $\tilde{\mathbf{R}}_k$ is the displacement of the deformed structure subjected to a unit displacement imposed at the kth support degree of freedom. Consequently, any quantity of interest (displacement, deformation, force,...) $\mathscr{E}$ in the structure which can be written as a linear combination of the above-mentioned degrees of freedom may also be expressed as a sum of pseudo-static and dynamic components:

$$\mathscr{E}(t) = \mathbf{D}^{\mathrm{T}} \begin{Bmatrix} \mathbf{Y} \\ \mathbf{Z} \end{Bmatrix} = \sum_{k=1}^{NS} a_k z_k(t) + \sum_{r=1}^{NM} \sum_{l=1}^{NS} b_l^r s_l^r(t) \tag{3}$$

where $a_k = \mathbf{D}^{\mathrm{T}} \tilde{\mathbf{R}}_k$ is the effect on the quantity $\mathscr{E}$ of an imposed unit displacement at support k and $b_l^r = \gamma_{rk} \mathbf{D}^{\mathrm{T}} \mathbf{\Phi}_r$ is the effect on $\mathscr{E}$ of the rth mode shape $\mathbf{\Phi}_r$ multiplied by a local participation factor:

$$\gamma_{rk} = -\frac{\mathbf{\Phi}_r^{\mathrm{T}} \mathbf{M}_{\mathrm{s}} \tilde{\mathbf{R}}_k}{\mathbf{\Phi}_r^{\mathrm{T}} \mathbf{M}_{\mathrm{s}} \mathbf{\Phi}_r} \tag{4}$$

Also, s_k^r satisfies:

$$\ddot{s}_k^r + 2\zeta_r \omega_r \dot{s}_k^r + \omega_r^2 s_k^r = \ddot{z}_k \tag{5}$$

z_k being the ground displacement at the kth support degree of freedom ($\mathbf{Z} = [z_1, z_2, \ldots z_{\mathrm{NS}}]^{\mathrm{T}}$). Der Kiureghian and Neuenhofer[15] derived a combination rule known as the multiple support response spectrum (MSRS) method, which yields approximately the mean maximum response:

$$(E[\mathscr{E}_{\max}])^2 = \sum_{k,l=1}^{NS} a_k a_l \rho_{z_k z_l} z_{k,\max} z_{l,\max} + 2 \sum_{r=1}^{NM} \sum_{k,l=1}^{NS} a_k b_l^r \rho_{z_k s_l^r} z_{k,\max} D_l(\omega_r, \zeta_r)$$
$$+ \sum_{r,s=1}^{NM} \sum_{k,l=1}^{NS} b_k^r b_l^s \rho_{s_k^r s_l^s} D_k(\omega_r, \zeta_r) D_l(\omega_s, \zeta_s) \tag{6}$$

in which $z_{k,\max}$ and $D_k(\omega_r, \zeta_r)$ are, respectively, the mean maximum ground displacement and the mean maximum relative displacement of an oscillator (ω_r, ζ_r) at support location k obtained from a linear response spectrum characteristic of the site. The correlation coefficients are obtained by random vibration analysis:

$$\rho_{z_k z_l} = \frac{\int_{-\infty}^{\infty} \omega^{-4} S_{\ddot{z}_k \ddot{z}_l}(\omega)\, \mathrm{d}\omega}{\sqrt{\int_{-\infty}^{\infty} \omega^{-4} S_{\ddot{z}_k}(\omega)\, \mathrm{d}\omega \cdot \int_{-\infty}^{\infty} \omega^{-4} S_{\ddot{z}_l}(\omega)\, \mathrm{d}\omega}}$$
$$\rho_{z_k s_l^r} = -\frac{\mathrm{Re}\left\{\int_{-\infty}^{\infty} \omega^{-2} h_r(\omega) S_{\ddot{z}_k \ddot{z}_l}(\omega)\, \mathrm{d}\omega\right\}}{\sqrt{\int_{-\infty}^{\infty} \omega^{-4} S_{\ddot{z}_k}(\omega)\, \mathrm{d}\omega \cdot \int_{-\infty}^{\infty} |h_r(\omega)|^2 S_{\ddot{z}_l}(\omega)\, \mathrm{d}\omega}}$$
$$\rho_{s_k^r s_l^s} = \frac{\int_{-\infty}^{\infty} h_r(-\omega) h_s(\omega) S_{\ddot{z}_k \ddot{z}_l}(\omega)\, \mathrm{d}\omega}{\sqrt{\int_{-\infty}^{\infty} |h_r(\omega)|^2 S_{\ddot{z}_k}(\omega)\, \mathrm{d}\omega \cdot \int_{-\infty}^{\infty} |h_s(\omega)|^2 S_{\ddot{z}_l}(\omega)\, \mathrm{d}\omega}} \tag{7}$$

where $S_{\ddot{z}_k}$ [resp. $S_{\ddot{z}_k \ddot{z}_l}$] designates the ground acceleration auto- [resp. cross] power spectral density and h_r the transfer function $h_r(\omega) = [\omega_r^2 - \omega^2 + 2\mathrm{i}\zeta_r \omega_r \omega]^{-1}$.

CHARACTERIZATION OF SPATIAL VARIABILITY

Assuming stationary processes and a homogeneous auto-power spectral density of ground acceleration $S_{\ddot{u}}(\omega)$, the cross-power spectral density of ground accelerations in a particular direction between surface points A and B may be written as:

$$S_{\ddot{u}_A \ddot{u}_B}(\omega) = \Gamma_{AB}(\omega) S_{\ddot{u}}(\omega) \tag{8}$$

The complex valued function $\Gamma_{AB}(\omega)$ accounts for the loss of coherency and phase delay between ground accelerations at point A and point B. Several models have been fitted to data obtained from arrays of strong motion recorders.[3–6] In this paper, the very simple functional shape is used:

$$\Gamma_{AB}(\omega) = \exp\left[-(\alpha \omega d_{AB})^2\right] \exp\left[-\mathrm{i}(\omega d_{AB}/V)\right] \tag{9}$$

If not very sophisticated, it leads however to a simple investigation of the influence on a bridge response of the seismic wave spatial variability. It was first derived by Uscinski[26] by solving the plane wave propagation

problem in a random medium and was also used by Luco and Wong.[4] Parameters α, V, and d_{AB} measure respectively the loss of coherency rate with distance and frequency, the apparent wave velocity (assumed constant for all frequencies), and the algebraic distance between surface points A and B. Note that d_{AB} and V can be positive or negative (an orientation along the bridge line must therefore be chosen) to describe the direction of propagation. Typical values of α range from 0 to 10^{-3} s/m and from approximately 200 m/s to infinity for V, depending on the angle of incidence of the seismic wave. The power spectral density used in the numerical computations is iteratively computed so that the maximum displacements of a dense set of oscillators best match a given elastic response spectrum.[23]

SENSITIVITY OF BRIDGES TO SMALL SPATIAL VARIATIONS OF GROUND MOTIONS

In the following derivation, the dimensionless quantities $\alpha\omega_1 l$ and $\omega_1 l/V$ (where ω_1 is the bridge fundamental frequency and l the bridge length) are assumed to be a lot smaller than unity. This indicates that the seismic motion varies in space slowly with respect to the bridge dimensions and dynamic characteristics. A single direction of seismic motion is considered, either longitudinal, lateral, or vertical. As a consequence, there is only one translation degree of freedom per foundation in vector $\mathbf{Z}$. It should be noted however, that this point of view implicitly assumes that the components of the ground motions are independent so that each direction of excitation may be analyzed separately. This might not always be the case, in particular in the low frequency range to which long bridges are sensitive and where surface waves may bring some degree of correlation between ground motion components. Also, some coupling between the effects of ground motion components may be introduced by the structure itself, e.g. between lateral and longitudinal ground motion effects for curved bridges, longitudinal and vertical for cable-stayed or suspension bridges. If models of correlation for different ground motion components are available, then the following simplified analysis is inappropriate and the complete MSRS rule (6) should be used. For the sake of clarity, pseudo-static and dynamic motions are assumed to be uncorrelated, which is justified if the fundamental frequency of the structure is larger than 0·5 Hz.[15] In addition, modal frequencies are assumed to be far apart so that cross-modal correlations may be disregarded (the SRSS rule is based on this assumption). The triple sum of equation (6) vanishes, and so do all cross terms ($r \neq s$) from the quadruple sum.

Based on the expansion of the coherency function, a second order-Taylor expansion of equation (6) with respect to α and $1/V$ can be derived (see Appendix I):

$$E[|\mathscr{E}_{\max}|]^2 = \left\{ \mathscr{E}_{\mathrm{U}}^2 u^2{}_{\max} + \sum_{r=1}^{NM} \gamma_r^2 \mathscr{E}_{\mathbf{\Phi}_r}^2 D(\omega_r, \zeta_r)^2 \right\}$$
$$+ \left(\alpha^2 + \frac{1}{2V^2} \right) \left\{ \Delta_0 \dot{u}^2{}_{\max} + \sum_{r=1}^{NM} \Delta_r V(\omega_r, \zeta_r)^2 \right\} \tag{10}$$

where $\mathscr{E}_{\mathrm{U}}$ is the effect on the quantity $\mathscr{E}$ of a static uniform ground translation (i.e. zero if $\mathscr{E}$ is an internal force or a relative displacement within the structure), $\mathscr{E}_{\mathbf{\Phi}_r}$ is the effect of modal shape $\mathbf{\Phi}_r$ and $\gamma_r = \sum_{k=1}^{NS} \gamma_{rk}$ is the classical participation factor used for uniform ground motions. Thus, the first line of equation (10) is simply the well known SRSS rule. The second line describes the effect of small spatial variability of seismic motions: $\dot{u}_{\max}$ is the maximum ground velocity, $V(\omega_r, \zeta_r)$ is the response spectrum in pseudo-velocity, and Δ_0 and Δ_r are the following coefficients:

$$\Delta_0 = 2 \left[\left(\sum_{k=1}^{NS} \bar{d}_{Ok} a_k \right)^2 - \left(\sum_{k=1}^{NS} a_k \right) \left(\sum_{k=1}^{NS} \bar{d}_{Ok}^2 a_k \right) \right] \tag{11}$$

$$\Delta_r = 2\mathscr{E}_{\mathbf{\Phi}_r}^2 \left[\left(\sum_{k=1}^{NS} \bar{d}_{Ok} \gamma_{rk} \right)^2 - \left(\sum_{k=1}^{NS} \gamma_{rk} \right) \left(\sum_{k=1}^{NS} \bar{d}_{Ok}^2 \gamma_{rk} \right) \right] \tag{12}$$

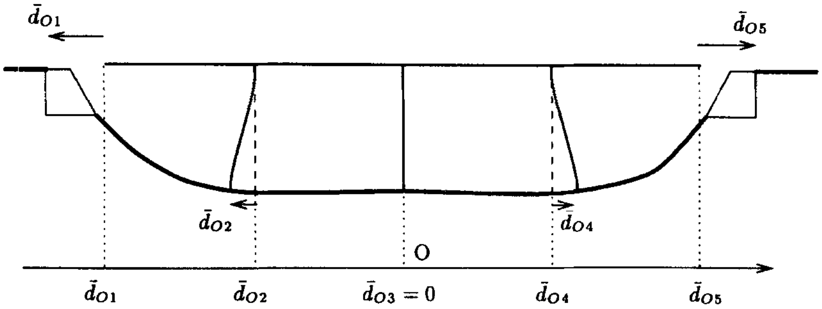

Figure 1. Static effect of a linear dilatation of the foundation soil (first order term for longitudinal ground motions)

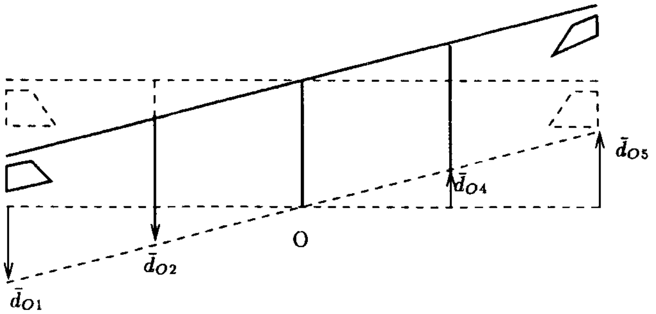

Figure 2. Static effect of a rotation of the foundation soil (first order term for lateral or vertical ground motions)

where $\bar{d}_{Ok}$ is the algebraic (positive or negative) distance from an arbitrary point O to support k measured on the bridge line (see Figure 1). Δ_0 and Δ_r are independent of the choice of point O. Assuming from now on, that $\mathscr{E}$ is an internal force (e.g. a bending moment or a shear force) or a relative displacement (e.g. the sliding of the bridge deck over a pier top), equation (10) modifies in the following way.

A static translation of the ground induces no internal force or relative displacement. Hence, $\mathscr{E}_{\mathrm{U}} = \sum_{k=1}^{NS} a_k = 0$ and

$$\Delta_0 = 2\left(\sum_{k=1}^{NS} \bar{d}_{Ok} a_k\right)^2 \tag{13}$$

which is positive and quantifies the increment in the pseudo-static component of the response. Note that Δ_0 is twice the square of the effect of a static spatial linear variation of ground displacements. If longitudinal displacements are considered, this linear variation is a dilatation or a contraction of the foundation soil along the bridge line (as shown in Figure 1) and therefore, efforts and/or relative displacements are generated ($\Delta_0 > 0$). Conversely, for lateral and vertical ground motions, the same linear variation of ground displacements represents a rigid rotation of the foundation soil (see Figure 2) and therefore, does not participate in the response ($\Delta_0 = 0$); in that case, the pseudo-static contribution is only of fourth order in α or $1/V$ and can be neglected. It is shown in Appendix II that the terms kept in the coherence function expansion do not account for any type of soil displacement curvature. This makes physical sense only if small spatial variations of ground motion are considered.

In the present work, we studied the bridge over the Gave de Pau, Lourdes, France. Figure 3 shows the first longitudinal mode and Figure 4 shows the first lateral swaying mode for this bridge.

The marginal dynamic response due to small spatial variations of ground motion is generally non-zero and its sign is that of the quantity:

$$\sum_{r=1}^{NM} \Delta_r V(\omega_r, \zeta_r)^2 \tag{14}$$

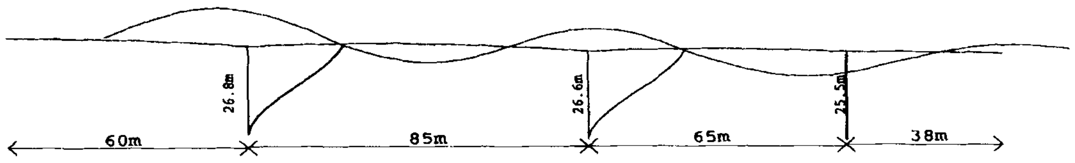

Figure 3. Bridge over the Gave de Pau, Lourdes, France: first longitudinal mode

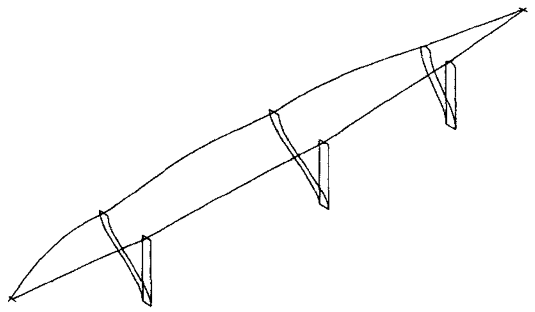

Figure 4. Bridge over the Gave de Pau, Lourdes, France: first lateral swaying mode

Note that anti-symmetrical modes of a symmetrical structure (such as modes 5, 21 and 39 of Figure 5) have a zero usual participation factor (i.e. $\gamma_r = \sum_{k=1}^{NS} \gamma_{rk} = 0$) and thus their contribution increases, as equation (12) shows, from zero to some strictly positive value. For symmetrical modes, investigation of real cases has shown that most of the time, Δ_r is negative, although no general rule can be asserted.

Also, if local participation factors γ_{rk} for a particular mode r all share the same sign, say positive, then with O chosen so that all $\bar{d}_{Ok}$ are positive, Schwarz's inequality ensures that Δ_r is negative and therefore the contribution of such a mode decreases with spatially varying seismic motions. This is guaranteed if the modal shape lies entirely on one side of the structure, which happens for example in the fundamental lateral swaying mode of a bridge on flexible piers (Figure 4). In that case, the total lateral dynamic response which is usually controlled by this fundamental mode is expected to decrease.

MODES TO BE KEPT IN THE ANALYSIS

In conventional seismic analysis, the effective modal mass is a commonly used criterion to assess how many and which modes should be used to properly describe the structural response. It is defined as:[25]

$$M^r = m_r \gamma_r^2 \tag{15}$$

where again only one direction of excitation is considered. It is recalled below that this quantity is a measure of the contribution of mode r in the total base shear force for uniform ground motions. It is well known that the sum of all the effective modal masses yields the total mass of the structure. Therefore, adding the effective modal mass of the modes included in the analysis gives an idea of how well the structural response is described. Now if non-synchronous seismic inputs are introduced in the model, the effective modal mass concept must be extended. In the following, the quality of the description of the driving forces is examined. From relations (1) and (2), one can extract the vector of the base shear forces (in the frequency domain):

$$\mathbf{F}(\omega) = \left[\mathbf{K}_{\mathrm{ff}} + \mathrm{i}\omega\mathbf{C}_{\mathrm{ff}} - \omega^2\mathbf{M}_{\mathrm{ff}}\right]\mathbf{Z}(\omega) + \left[\mathbf{K}_{\mathrm{sf}}^{\mathrm{T}} + \mathrm{i}\omega\mathbf{C}_{\mathrm{sf}}^{\mathrm{T}} - \omega^2\mathbf{M}_{\mathrm{sf}}^{\mathrm{T}}\right]\mathbf{X}(\omega) \tag{16}$$

where

$$\mathbf{K}_{\mathrm{ff}} = \mathbf{K}_{\mathrm{f}} - \mathbf{K}_{\mathrm{sf}}^{\mathrm{T}}\mathbf{K}_{\mathrm{s}}^{-1}\mathbf{K}_{\mathrm{sf}}, \qquad \mathbf{C}_{\mathrm{ff}} = \mathbf{C}_{\mathrm{f}} - \mathbf{C}_{\mathrm{sf}}^{\mathrm{T}}\mathbf{K}_{\mathrm{s}}^{-1}\mathbf{K}_{\mathrm{sf}}, \qquad \mathbf{M}_{\mathrm{ff}} = \mathbf{M}_{\mathrm{f}} - \mathbf{M}_{\mathrm{sf}}^{\mathrm{T}}\mathbf{K}_{\mathrm{s}}^{-1}\mathbf{K}_{\mathrm{sf}} \tag{17}$$

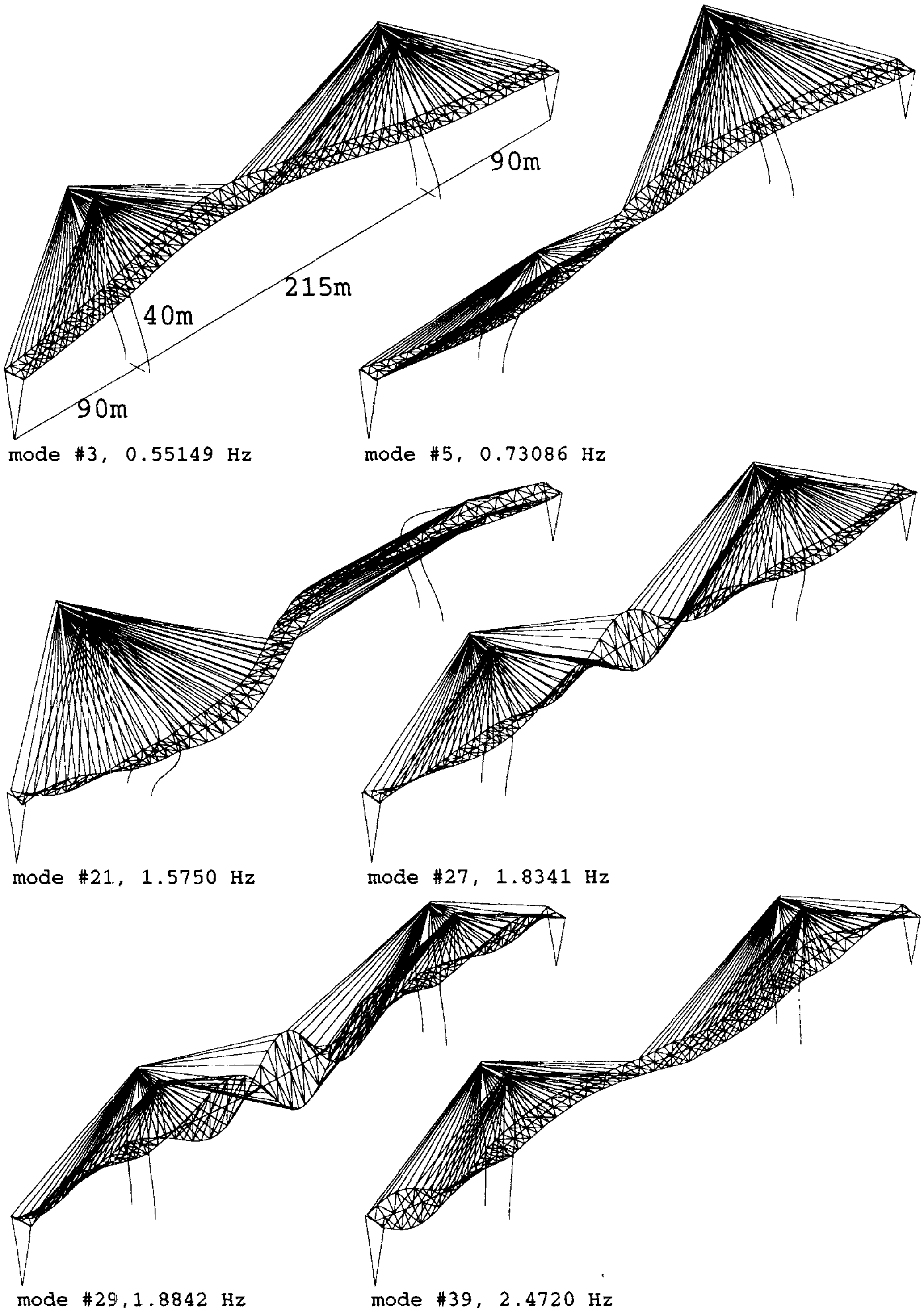

Figure 5. Evrypos cable-stayed bridge in Greece: modes controlling the lateral response

Neglecting the damping and mass effects due to the foundation and its coupling with the structure in front of the rigidity effect, equation (16) reduces to:

$$\mathbf{F}(\omega) = \mathbf{K}_{\mathrm{ff}}\mathbf{Z}(\omega) + \mathbf{K}_{\mathrm{sf}}^{\mathrm{T}}\mathbf{X}(\omega) \tag{18}$$

The purely dynamic part of the response can be expanded on the basis of the complete set of all NM modes as:

$$\mathbf{X}(\omega) = \sum_{r=1}^{NM}\sum_{k=1}^{NS} \gamma_{rk} s_k^r(\omega)\boldsymbol{\phi}_r \tag{19}$$

and since

$$\mathbf{K}_{\mathrm{sf}}^{\mathrm{T}}\boldsymbol{\phi}_r = (-\mathbf{K}_{\mathrm{sf}}^{\mathrm{T}}\mathbf{K}_{\mathrm{s}}^{-1})(-\mathbf{K}_{\mathrm{s}}\boldsymbol{\phi}_r) = \tilde{\mathbf{R}}^{\mathrm{T}}(-\omega_r^2\mathbf{M}_{\mathrm{s}}\boldsymbol{\phi}_r) = \omega_r^2 m_r\left[\gamma_{r,1}\cdots\gamma_{r,NS}\right]^{\mathrm{T}} \tag{20}$$

the lth base shear force F_l ($\mathbf{F} = [F_1 \cdots F_{NS}]^{\mathrm{T}}$) is given by:

$$F_l(\omega) = \sum_{k=1}^{NS} \mathbf{K}_{\mathrm{ff},lk}\, z_k(\omega) + \sum_{r=1}^{NM}\sum_{k=1}^{NS} m_r\gamma_{rl}\gamma_{rk}\left(\omega_r^2 s_k^r(\omega)\right) \tag{21}$$

Among all possible seismic motion correlation patterns, the extreme cases of uniform ground motion and total loss of coherency are considered hereafter.

1. Uniform ground motion: $z_k(\omega) = z(\omega)$ and the pseudo-static term vanishes (indeed, $\sum_{k=1}^{NS}\mathbf{K}_{\mathrm{ff},lk} = 0$). Also, the dynamic term reduces to:

$$F_l(\omega) = \sum_{r=1}^{NM} m_r\gamma_{rl}\gamma_r\left(\omega_r^2 s_k^r(\omega)\right) \tag{22}$$

   where $\gamma_r = \sum_{k=1}^{NS}\gamma_{rk}$. The total shear force is then:

$$F(\omega) = \sum_{l=1}^{NS} F_l(\omega) = \sum_{r=1}^{NM} m_r\gamma_r^2\left(\omega_r^2 s_k^r(\omega)\right) \tag{23}$$

   hence, neglecting the cross-modal correlations, the squared expected maximum total shear force is

$$E\left[|F|_{\max}\right]^2 = \sum_{r=1}^{NM}(m_r\gamma_r^2)^2(A(\omega_r,\zeta_r))^2 \tag{24}$$

   where $A(\omega_r,\zeta_r)$ is the elastic response in pseudo-acceleration. The usual effective modal mass naturally appears here and is an indicator of how important the modal contribution is in the total response, regardless of the input spectral content.
2. Totally incoherent support motions: the correlation coefficients (7) are

$$\rho_{z_k z_l} = \delta_{kl}, \qquad \rho_{z_k s_l^r} = 0, \qquad \rho_{s_k^r s_l^s} = \delta_{kl}\delta_{rs} \quad (\delta_{ij} = 1 \text{ if } i = j \text{ and } 0 \text{ otherwise}) \tag{25}$$

   where statistical independence has been assumed between pseudo-static and dynamic motions, and between cross-modal responses. The expected maximum value of each support force turns out to be:

$$E\left[|F_l|_{\max}\right]^2 = \sum_{k=1}^{NS}(\mathbf{K}_{\mathrm{ff},lk})^2 z_{\max}^2 + \sum_{r=1}^{NM}\sum_{k=1}^{NS}(m_r\gamma_{rl}\gamma_{rk})^2 A(\omega_r,\zeta_r)^2 \tag{26}$$

   Eventually, summing up individual mean maximum forces over the whole set of supports yields:

$$\sum_{l=1}^{NS} E\left[|F_l|_{\max}\right]^2 = \left[\sum_{k,l=1}^{NS}(\mathbf{K}_{\mathrm{ff},lk})^2\right] z_{\max}^2 + \sum_{r=1}^{NM}\left[m_r\sum_{k=1}^{NS}\gamma_{rk}^2\right]^2 A(\omega_r,\zeta_r)^2 \tag{27}$$

An effective modal mass for totally incoherent ground motions M_{TI}^{r} is thus naturally introduced as:

$$M_{\mathrm{TI}}^{r} = m_r \sum_{k=1}^{NS} \gamma_{rk}^2 \tag{28}$$

Noting that since $\tilde{\mathbf{R}}_k = \sum_{r=1}^{NM} \gamma_{rk} \boldsymbol{\phi}_r$ one has $\tilde{\mathbf{R}}_k^{\mathrm{T}} \mathbf{M}_{\mathrm{s}} \tilde{\mathbf{R}}_k = \sum_{r=1}^{NM} m_r \gamma_{rk}^2$ and therefore

$$\sum_{k=1}^{NS} \tilde{\mathbf{R}}_k^{\mathrm{T}} \mathbf{M}_{\mathrm{s}} \tilde{\mathbf{R}}_k = \sum_{r=1}^{NM} M_{\mathrm{TI}}^{r} \tag{29}$$

The left-hand side of the above equation, from now on called the sum of the 'pseudo-static masses', can be easily computed, just like the total mass of the structure $\mathbf{U}^{\mathrm{T}} \mathbf{M}_{\mathrm{s}} \mathbf{U}$, where $\mathbf{U}$ is a unit translation vector.

Since lower modes usually contain most of the response, it is common practice to truncate the modal expansion to a small number of modes ($NM' \ll NM$). As far as base shear forces are concerned, the truncation can be justified in the above extreme cases by the following ratios:

1. The ratio of the sum of the effective modal masses over the total mass of the structure:

$$r_{\mathrm{TC}} = \frac{\sum_{r=1}^{NM'} M^r}{M_{\mathrm{T}}} \tag{30}$$

indicates how well the base forces are described in case of uniform ground motions. The closer the ratio is to unity, the more complete is the modal basis.

2. Similarly, the ratio of the sum of the effective modal masses for totally incoherent ground motions over the sum of the 'pseudo-static masses':

$$r_{\mathrm{TI}} = \frac{\sum_{r=1}^{NM'} M_{\mathrm{TI}}^{r}}{\sum_{k=1}^{NS} \tilde{\mathbf{R}}_k^{\mathrm{T}} \mathbf{M}_{\mathrm{s}} \tilde{\mathbf{R}}_k} \tag{31}$$

indicates how well the base forces are described in case of totally incoherent ground motions.

Indeed, the truncation error in equation (24) is:

$$err_{NM'} = \sum_{r=NM'+1}^{NM} (M^r A(\omega_r, \zeta_r))^2 \tag{32}$$

and since the pseudo-acceleration is a decreasing function for high frequencies,

$$err_{NM'} \leqslant (M_{\mathrm{T}} A(\omega_{NM'}, \zeta_{NM'}))^2 \sum_{r=NM'+1}^{NM} \left(\frac{M^r}{M_{\mathrm{T}}}\right)^2 \leqslant (M_{\mathrm{T}} A(\omega_{NM'}, \zeta_{NM'}))^2 \sum_{r=NM'+1}^{NM} \frac{M^r}{M_{\mathrm{T}}} \tag{33}$$

or

$$err_{NM'} \leqslant (M_{\mathrm{T}} A(\omega_{NM'}, \zeta_{NM'}))^2 (1 - r_{\mathrm{TC}}) \tag{34}$$

Similarly for totally incoherent ground motions, the truncation error of equation (27) is bounded by:

$$err_{NM'} \leqslant \left(\sum_{k=1}^{NS} \tilde{\mathbf{R}}_k^{\mathrm{T}} \mathbf{M}_{\mathrm{s}} \tilde{\mathbf{R}}_k\right)^2 A(\omega_{NM'}, \zeta_{NM'})^2 (1 - r_{\mathrm{TI}}) \tag{35}$$

Note that for all intermediate cases between totally coherent and totally incoherent ground motions, an upper bound of the truncation error can also be found (see Appendix III). It turns out that the closer to unity

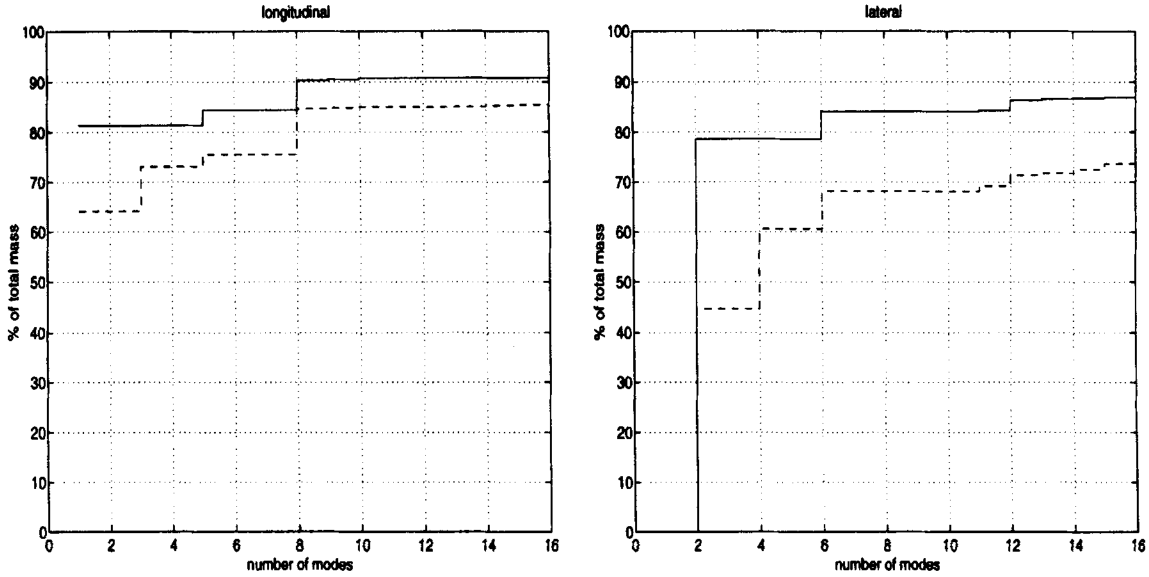

Figure 6. Bridge over the Gave de Pau. Cumulative effective modal mass. Solid line: uniform ground motions ($r_{TC} \times 100$). Dashed line: totally incoherent ground motions ($r_{TI} \times 100$). Longitudinal ground motions (left) and lateral ground motions (right)

r_{TI} comes, the smaller the truncation error is. Figure 6 shows both ratios r_{TC} and r_{TI}: r_{TC} converges faster to unity than r_{TI} showing that more modes must be included to account for the effect of spatial variations of earthquake motions.

CASE STUDIES OF REAL BRIDGES

In this section, the results of the sensitivity analysis and the approximate formula (10) are examined in the light of numerical examples run on finite element models of real bridges. All computations are carried out according to the MSRS rule (equation (6)) and the approximate formula (10), using the recommendation of the French Earthquake Engineering Association (AFPS) for the elastic response spectrum on rock $D(\omega, \zeta)$ (with a maximal ground acceleration of $1\,\mathrm{m/s^2}$). The power spectral density used to compute the cross-correlation coefficients are chosen to best fit the given response spectrum.[23]

Longitudinal ground motions

As mentioned above, for longitudinal ground excitations, the terms to be kept in expression (10) are:

$$E[|\mathscr{E}_{\max}|]^2 = \sum_{r=1}^{NM} \gamma_r^2 \mathscr{E}_{\Phi_r}^2 D(\omega_r, \zeta_r)^2 + \left(\alpha^2 + \frac{1}{2V^2}\right)\left\{\Delta_0 \dot{u}^2{}_{\max} + \sum_{r=1}^{NM} \Delta_r V(\omega_r, \zeta_r)^2\right\} \tag{36}$$

It is known from equation (13) that the pseudo-static contribution increases the response. Figure 3 shows that the fundamental mode is usually of constant sign, as far as longitudinal movements are concerned. Therefore, the spatial variability of seismic motions decreases its contribution to the response. Essentially, the sign of the change in the total response $\mathscr{E}$ results from a trade-off between the pseudo-static term $\Delta_0 \dot{u}^2_{\max}$ and the marginal contribution $\Delta_1 V(\omega_1, \zeta_1)^2$ of the fundamental longitudinal swaying mode.

Figure 7 shows the maximum central pier base shear force and the maximum deck-over-abutment sliding for the bridge over the Gave de Pau (Lourdes, France) subjected to longitudinal ground motions. The maximum responses are presented for a range of spatial loss of coherency of the earthquake excitation ($0 \leqslant \alpha \leqslant 2 \times 10^{-3}$) as computed by the complete MSRS rule and the approximate formula (10). The fundamental longitudinal mode (Figure 3) has a frequency of $f_1 = 0{\cdot}87\,\mathrm{Hz}$. Since the bridge length is $L = 248\,\mathrm{m}$, the approximation

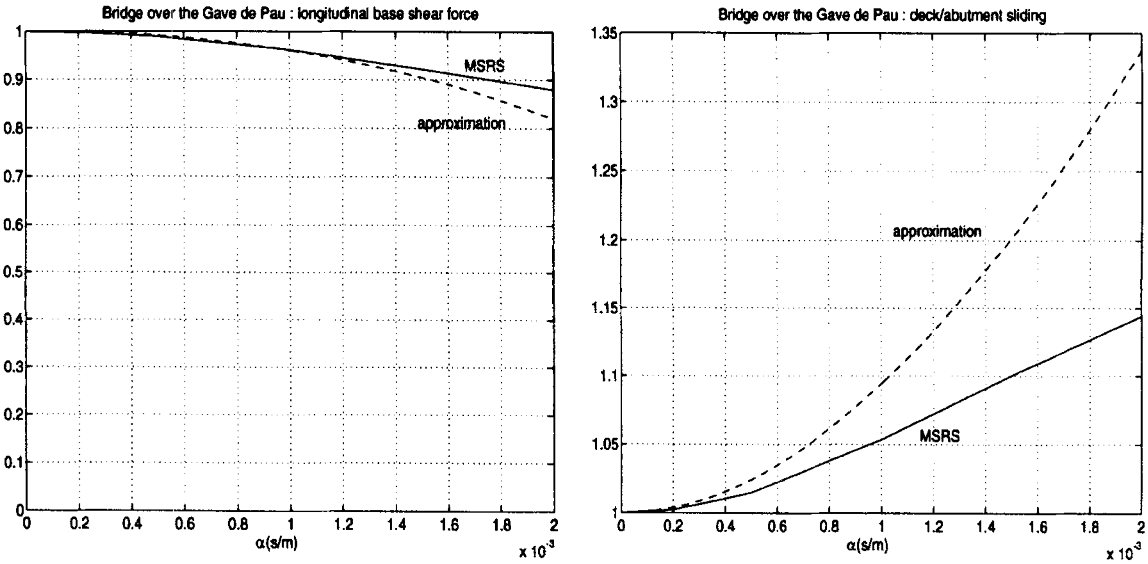

Figure 7. Bridge over the Gave de Pau. Longitudinal ground motions: central pier base shear force (left) and deck/abutment sliding (right)

is not expected to be accurate for values of α over $1/(2\pi f_1 L) = 0{\cdot}74 \times 10^{-3}$ s/m (recall that a necessary assumption for the approximation to hold is that $\alpha\omega_1 L$ and $\omega_1 L/V$ be smaller than unity). The approximation is still quite accurate beyond that value for the base shear force, however the discrepancy shown for the deck/abutment sliding forbids the use of the approximate formula for large spatial variability conditions. The trend of the variation is however indicated clearly by the approximate formula and in particular by the sign of the quantity $\Delta_0 \dot{u}^2_{\max} + \sum_{r=1}^{NM} \Delta_r V(\omega_r, \zeta_r)^2$: positive for the deck/abutment sliding, leading to an increasing response with spatial variability and negative for the base shear force, leading to a decreasing response.

Lateral ground motions

As mentioned earlier, the pseudo-static contribution generated by lateral and vertical ground motions vanishes from the second order expansion of equation (36) where only the dynamic contribution remains:

$$E[|\mathscr{E}_{\max}|]^2 = \sum_{r=1}^{NM} \gamma_r^2 \mathscr{E}_{\Phi_r}^2 D(\omega_r, \zeta_r)^2 + \left(\alpha^2 + \frac{1}{2V^2}\right)\left\{\sum_{r=1}^{NM} \Delta_r V(\omega_r, \zeta_r)^2\right\} \tag{37}$$

If the first swaying mode (shown in Figure 4) dominates lateral movements of the bridge, then as it is entirely on one side of the bridge position at rest, its local participation factors share the same sign and the response decreases.

Figure 8 shows that the spatial variation of ground motions indeed diminishes the base shear force of the center pier for the bridge over the Gave de Pau and the Evrypos bridge base shear force. In the case of the bridge over the Gave de Pau, the fundamental lateral swaying mode has a frequency of $f_1 = 1{\cdot}06$ Hz, limiting the meaningful range of the approximation to $\alpha \leqslant 6 \times 10^{-4}$ s/m. Beyond that, the error between the approximate formula and the MSRS rule becomes significant.

Note, however, that there is no particular reason to believe that most of the marginal dynamic contribution comes from the first lateral mode. In fact, for the Evrypos cable-stayed bridge (Greece), the pier base shear force generated by lateral ground motions results mainly from the six modes shown in Figure 5, (as can be seen from the Δ_r's). Figure 8 shows that the discrepancy between the MSRS rule and the approximate formula is very large for this bridge. One reason for this is that some of the concerned frequencies violate the restriction $\alpha\omega_r L \ll 1$, even for very small values of α. Another reason that can be observed even for $\alpha = 0$, is that there is a significant amount of coupling between modes (some of the eigenfrequencies are closely spaced) which is not taken into account in the approximate formula (10).

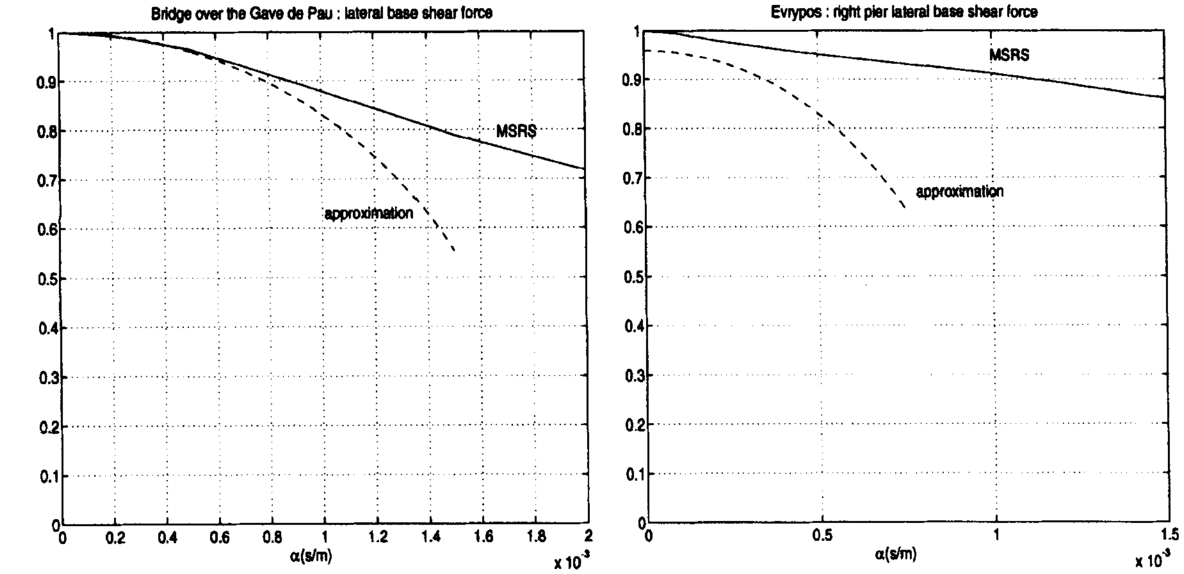

Figure 8. Lateral ground motions, central pier base shear force: bridge over the Gave de Pau (left), Evrypos bridge (right)

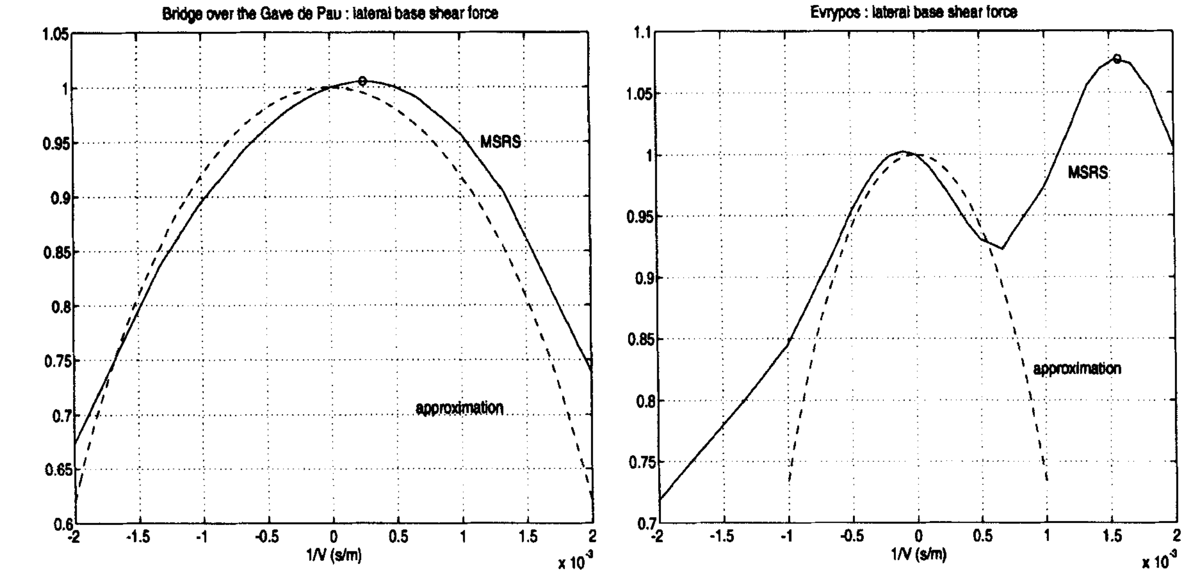

Figure 9. Lateral ground motions. Effect of the wave passage effect on the base shear force of the bridge over the Gave de Pau central pier (left) and of the Evrypos bridge right pier ($V > 0$ when propagating from left to right)

It is important to note that the wave passage phenomenon has a dissymmetrical effect due to the coupling between modal responses[23] which the Taylor expansion does not account for. Figure 9 shows that the dissymmetry of the response given by the MSRS rule and the discrepancy with the approximation can be of significant importance, in particular in the case of the Evrypos bridge pylon base shear force. A general method to deal with large and unknown spatial variations of seismic waves is presented further down in this paper.

Vertical ground motions

For vertical seismic motions, equation (37) still holds. The quantities that are of most interest are bending moments and vertical shear forces in the bridge deck. Since piers are very rigid in compression, the problem

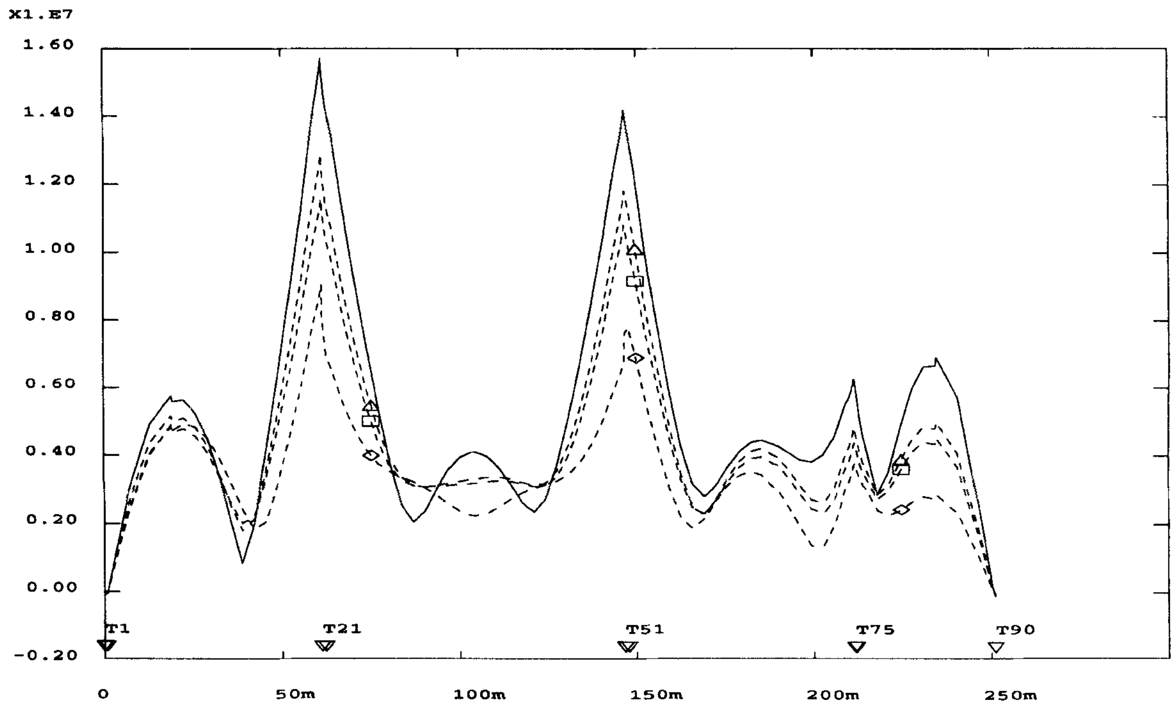

Figure 10. Vertical seismic motions:bending moment along the bridge deck. The four span bridge over the Gave de Pau. △: $\alpha = 10^{-3}$ s/m, $V = \infty$; ◇: $\alpha = 2\cdot 10^{-3}$ s/m, $V = \infty$; □: $\alpha = 0$, $V = 500$ m/s

is actually that of a multiply supported beam if the deck is free to rotate at the supports, otherwise one must include rotational springs accounting for the bending of the piers.

If the bridge is made of statically determinate simply supported spans, then each span may be studied independently; in such a case, it has been shown[8] that spatially varying seismic motions decrease the bridge response mainly because the latter is governed by the first one-sided flexural mode.

The situation is slightly more complex for multi-span indeterminate bridges and depends on the rigidity of the beam.[13,15] For rigid body vertical translations of the ground, the modes that are most excited are those that have a deformed shape that stays on one side of the bridge line; actually, the usual participation factor decreases rapidly when the modal shape alternates above and below the bridge line. For these one-sided modes, the bending moment is usually the highest at the support location, the mode shape showing its highest curvature there. For alternating modes, the maximum bending moments usually lie away from the support location. With increasing spatial variability of seismic waves, the bending moment at a support is therefore expected to diminish (along with a decreasing contribution of one-sided modes) but no conclusion can be drawn for the rest of the span. Figure 10 illustrates this fact for a continuous prestressed concrete bridge: bending moments are plotted along the bridge line for the usual rigid ground motion (solid curve) and three cases of spatial variability (dashed curves): $\alpha = 10^{-3}$ s/m and $V = \infty$, $\alpha = 2 \times 10^{-3}$ s/m and $V = \infty$, $\alpha = 0$ and $V = 500$ m/s. Support locations are marked with downward pointing triangles ($\bigtriangledown$). The vertical shear forces do not exhibit any particular trend.

LARGE AND/OR UNKNOWN SPATIAL VARIATIONS OF EARTHQUAKE MOTIONS

When seismic waves spatial variability is large with respect to the bridge dynamic characteristics or when cross-modal correlations are significant, the preceding approximate solution fails to yield an accurate value or trend for the maximum expected response. Also, spatial variability model parameters may not be known precisely or may be known only to reside in a given domain. If, for instance, the direction of propagation of seismic waves is unknown, the apparent wave velocity can range from the wave velocity in the bedrock (if the

waves propagate along the bridge line) to infinity (if waves propagate perpendicular to that line). Similarly, the loss of coherency rate (α) may be uncertain, possibly restricted to an interval, the bounds of which are based on empirical knowledge. In order to be on the safe side, it is desirable to compute the maximum of the mean peak response (6) when model parameters vary freely in the aforementioned domain. For a given spatial variability model (e.g. the one prescribed by the coherency function (9)), the correlation coefficients as well as the mean peak response (6) are highly nonlinear although smooth functions of the model parameters. There are very effective numerical methods to find the maximum value of nonlinear functions if the first and second derivatives are available. In the following, it is shown that the derivatives of the mean peak response with respect to the spatial variability model parameters may be computed simultaneously with the response itself, at little extra cost.

Derivatives of the maximum response

To compute the first and second derivatives of the mean peak response (6), one needs the derivatives of the correlation coefficients (7) and therefore those of the coherency function (9) with respect to the spatial variability parameters. In our example, the parameters may be chosen to be α and $1/V$ so that the first derivatives are:

$$\frac{\partial \Gamma_{AB}}{\partial \alpha}(\omega) = -2\alpha(\omega d_{AB})^2 \Gamma_{AB}(\omega), \qquad \frac{\partial \Gamma_{AB}}{\partial (1/V)}(\omega) = -\mathrm{i}\omega d_{AB} \Gamma_{AB}(\omega) \tag{38}$$

and the second derivatives

$$\frac{\partial^2 \Gamma_{AB}}{\partial \alpha^2}(\omega) = 2(\omega d_{AB})^2 \left\{ 2(\alpha \omega d_{AB})^2 - 1 \right\} \Gamma_{AB}(\omega), \qquad \frac{\partial^2 \Gamma_{AB}}{\partial (1/V)^2}(\omega) = -(\omega d_{AB})^2 \Gamma_{AB}(\omega) \tag{39}$$

$$\frac{\partial^2 \Gamma_{AB}}{\partial \alpha \partial (1/V)}(\omega) = 2\mathrm{i}\alpha(\omega d_{AB})^3 \Gamma_{AB}(\omega)$$

The derivatives of the correlation coefficients follow immediately by replacing the expression of Γ by its derivatives in the cross power spectral density (equation (8)) and then in the numerator of (7). The correlation coefficients are computed numerically (see for example the integration scheme suggested in Reference 14) and simultaneously their derivatives can be computed at very little extra cost.

Maximum response

In the following, $\hat{\mathscr{E}}(\underline{\theta})$ designate the mean peak response (6) for a vector $\underline{\theta}$ of κ variability parameters. In the vicinity of a set of parameters $\underline{\theta}^0$, the second order Taylor expansion of the response writes:

$$\hat{\mathscr{E}}(\underline{\theta}) = \hat{\mathscr{E}}(\underline{\theta}^0) + \nabla \hat{\mathscr{E}} \underline{\delta\theta} + \frac{1}{2} \underline{\delta\theta}^{\mathrm{T}} \mathscr{H} \underline{\delta\theta} \tag{40}$$

where $\underline{\delta\theta} = \underline{\theta} - \underline{\theta}^0$, $\nabla \hat{\mathscr{E}}$ designates the gradient and $\mathscr{H}$ the Hessian matrix:

$$\nabla \hat{\mathscr{E}} = \left[\frac{\partial \hat{\mathscr{E}}}{\partial \theta_1} \; \frac{\partial \hat{\mathscr{E}}}{\partial \theta_2} \cdots \frac{\partial \hat{\mathscr{E}}}{\partial \theta_\kappa} \right], \qquad \mathscr{H}_{i,j} = \left[\frac{\partial^2 \hat{\mathscr{E}}}{\partial \theta_i \partial \theta_j} \right] \tag{41}$$

$\mathscr{H}$ is a small symmetrical matrix (there are usually only a few parameters) that can be easily diagonalized as:

$$\mathbf{P}^{\mathrm{T}} \mathscr{H} \mathbf{P} = \operatorname{diag} \left\{ \lambda_1 \; \lambda_2 \cdots \lambda_\kappa \right\} \tag{42}$$

where $\mathbf{P}$ is an orthonormal matrix of eigenvectors $\mathbf{P} = [\mathbf{P}_1 | \mathbf{P}_2 | \cdots | \mathbf{P}_\kappa]$. Each eigenvector lies in the direction of a principal curvature. The λ_i's are the principal curvatures. Define the transformed set of parameters variations

$\underline{\delta\xi} = \mathbf{P}^{\mathrm{T}}\underline{\delta\theta}$. Equation (40) now writes:

$$\hat{\mathscr{E}} = \hat{\mathscr{E}}^0 + \sum_{i=1}^{K}(\nabla\hat{\mathscr{E}}\,.\,\mathbf{P}_i)\delta\xi_i + \frac{1}{2}\sum_{i=1}^{K}\lambda_i(\delta\xi_i)^2 \tag{43}$$

In the search for a maximum, each transformed variable can be dealt with independently. If equation (43) were a global identity, a maximum could only be found if all curvatures λ_i's were negative, the solution being given by the following set of transformed parameter variations: $\delta\xi_i = -(\nabla\hat{\mathscr{E}}\,.\,\mathbf{P}_i)/\lambda_i$. Since (43) is only a local approximation, the following strategy is adopted in each principal direction:

(1) If $\lambda_i < 0$ then $\delta\xi_i = -(\nabla\hat{\mathscr{E}}\,.\,\mathbf{P}_i)/\lambda_i$ (to reach a local maximum in that direction) or $\delta\xi_i = \mathrm{sign}(\nabla\hat{\mathscr{E}}\,.\,\mathbf{P}_i)\delta\xi_{\max}$ (to go upward) whichever is smaller in absolute value.
(2) If $\lambda_i \geqslant 0$ then $\delta\xi_i = \mathrm{sign}\,(\nabla\hat{\mathscr{E}}\,.\,\mathbf{P}_i)\delta\xi_{\max}$ (to go up in that direction)

where $\delta\xi_{\max}$ is a prescribed maximum step-size. Also, back in the original space ($\underline{\delta\theta} = \mathbf{P}\underline{\delta\xi}$), the physical parameters ($\underline{\theta} = \underline{\theta}^0 + \underline{\delta\theta}$) may be forced to remain within certain bounds prescribed by the physics (e.g. $\alpha \geqslant 0$, $|V| \geqslant$ shear wave velocity in the bedrock) or empirical knowledge. The MSRS response is computed for the new set of spatial variability model parameters along with the first and second derivatives. This step is repeated until the marginal change in the parameter values drops below a prescribed tolerance.

Numerical results

The method is applied to find the maximum pier base shear force of the two bridges examined above. The parameters α and V of the spatial variability model (9) are bounded in the following way:

$$0 \leqslant \alpha \leqslant 2 \times 10^{-3}\,\mathrm{s/m} \qquad \text{and} \qquad |V| \geqslant 200\,\mathrm{m/s} \tag{44}$$

The maxima thus found are marked on Figure 9 by little circles. The Evrypos right pier base shear force response warns against a possible pitfall: there is no reason for a maximum found by the preceding procedure to be a global maximum. Therefore, it is advisable to start the iterative procedure from several different sets of initial model parameters.

CONCLUSIONS

The sensitivity of bridges to small spatial variations of seismic waves is analyzed within the framework of multiple-support spectral analysis. The marginal pseudo-static and dynamic contributions are estimated analytically. Although only valid for small spatial variations of seismic motions, the analytical derivation gives some insight into the bridge response and may therefore be used at a preliminary design stage. It is shown that for relative displacements or internal forces the pseudo-static contribution is only influenced by spatial variations of longitudinal seismic motions and not by spatial variations of lateral or vertical ground motions. The influence of modal shapes on the dynamic contribution is also discussed: the seismic waves' spatial variability decreases the contribution of modes with shapes lying on one side of the structure at rest and increases that of anti-symmetrical modes. A criterion is given to assess the sensitivity of other modes and the completeness of the modal basis used in the analysis.

For larger spatial variations of earthquake induced ground motions that are, besides, only known to be confined within a given range, an algorithm is proposed to find the maximum mean peak response as given by the complete MSRS combination rule. It is based on the computation of the first and second derivatives of the mean peak response with respect to the parameters of the spatial variability model. The computation of the derivatives is carried out simultaneously with the computation of the response, at little extra cost.

In earthquake engineering, most of the uncertainties come from the ground motions. Very little is known in terms of spatial variability except in very well instrumented areas. The tools presented in this paper will allow the engineer to tackle the problem in a pragmatic way.

ACKNOWLEDGEMENTS

All finite element computations were carried out using the CASTEM 2000 code of the Commissariat à l'Energie Atomique. The authors wish to thank Messrs E. Conti (Service d'Etudes Techniques des Routes et Autoroutes) and J.M. Tourtois (GTM BTP Grands Travaux de Marseille) for supplying the finite element models used in this study and Professors A. Der Kiureghian, E. Kausel and Dr. A. Neuenhofer for their useful comments and indications.

APPENDIX I: DERIVATION OF THE SECOND ORDER APPROXIMATION

In the MSRS expression (6), it is first assumed that modal cross-correlations are negligible. It is well known that this assumption is only valid if modal frequencies lie sufficiently apart from one another. Der Kiureghian and Neuenhofer[23] have also shown that it can also be invalidated in the case of a wave propagating with very slow velocity. For eigenfrequencies above 0·5 Hz the correlation between pseudo-static and dynamic components is negligible.[23] Thus, for well spaced frequencies above 0·5 Hz, large apparent wave velocities and similar ground motions under all piers, the following holds approximately:

$$(E[\mathscr{E}_{\max}])^2 = \sum_{k,l=1}^{NS} a_k a_l \rho_{z_k z_l} u_{\max}^2 + \sum_{r}^{NM} \sum_{k,l=1}^{NS} b_k^r b_l^r \rho_{s_k^r s_l^r} D(\omega_r, \zeta_r)^2 \tag{45}$$

Now define σ_u and σ_r as:

$$\sigma_u^2 = \int_{-\infty}^{+\infty} S_{\ddot{u}}(\omega) \frac{\mathrm{d}\omega}{\omega^4}, \qquad \sigma_r^2 = \int_{-\infty}^{+\infty} |h_r(\omega)|^2 S_{\ddot{u}}(\omega)\, \mathrm{d}\omega \tag{46}$$

Based on the assumed variability model (9), the correlation coefficients of equation (45) can be written as

$$\begin{aligned}\rho_{z_k z_l} &= \frac{1}{\sigma_u^2} \int_{-\infty}^{+\infty} \exp\left(-(\alpha\omega d_{kl})^2 - \mathrm{i}\frac{\omega d_{kl}}{V}\right) S_{\ddot{u}}(\omega) \frac{\mathrm{d}\omega}{\omega^4} \\ \rho_{s_k^r s_l^r} &= \frac{1}{\sigma_r^2} \int_{-\infty}^{+\infty} \exp\left(-(\alpha\omega d_{kl})^2 - \mathrm{i}\frac{\omega d_{kl}}{V}\right) |h_r(\omega)|^2 S_{\ddot{u}}(\omega)\, \mathrm{d}\omega\end{aligned} \tag{47}$$

Now expand the coherency function:

$$\exp\left(-(\alpha\omega d_{kl})^2 - \mathrm{i}\frac{\omega d_{kl}}{V}\right) = 1 - \mathrm{i}\frac{\omega d_{kl}}{V} - \left(\alpha^2 + \frac{1}{2V^2}\right)(\omega d_{kl})^2 + 2\mathrm{i}\frac{\alpha^2}{V}(\omega d_{kl})^3 + \cdots \tag{48}$$

Since the rest of the integrand in equations (47) are real even functions of ω, the odd imaginary terms in the expansion (48) vanish (it would not be the case if cross-modal terms had been kept) and we are left with:

$$\begin{aligned}(E[\mathscr{E}_{\max}])^2 = {} & \left(\sum_{k}^{NS} a_k\right)^2 u_{\max}^2 + \sum_{r}^{NM} \left(\sum_{k}^{NS} b_k^r\right)^2 D(\omega_r, \zeta_r)^2 \\ & - \left(\alpha^2 + \frac{1}{2V^2}\right) \left\{ \sum_{k,l=1}^{NS} a_k a_l d_{kl}^2 \frac{u_{\max}^2}{\sigma_u^2} \int_{-\infty}^{+\infty} S_{\ddot{u}}(\omega) \frac{\mathrm{d}\omega}{\omega^2} \right. \\ & \left. + \sum_{r}^{NM} \sum_{k,l=1}^{NS} b_k^r b_l^r d_{kl}^2 \frac{D(\omega_r, \zeta_r)^2}{\sigma_r^2} \int_{-\infty}^{+\infty} \omega^2 |h_r(\omega)|^2 S_{\ddot{u}}(\omega) \mathrm{d}\omega \right\}\end{aligned} \tag{49}$$

Now define:

$$\mathscr{E}_{\mathrm{U}} = \sum_{k}^{NS} a_k = \mathbf{D}^{\mathrm{T}} \sum_{k}^{NS} \tilde{\mathbf{R}}_k = \mathbf{D}^{\mathrm{T}}\mathbf{U} \tag{50}$$

where $\mathbf{U}$ is the unit displacement of the whole structure. $\mathscr{E}_{\mathrm{U}}$ is the static effect on the structure of an imposed unit rigid displacement of the foundation system. If $\mathscr{E}$ is an effort or a relative displacement within the structure, then clearly $\mathscr{E}_{\mathrm{U}} = 0$. Also,

$$\sum_{k}^{NS} b_k^r = \left(\sum_{k}^{NS} \gamma_{rk}\right) \mathbf{D}^{\mathrm{T}}\boldsymbol{\Phi}_r = \gamma_r \mathscr{E}_{\boldsymbol{\Phi}_r} \tag{51}$$

where $\mathscr{E}_{\boldsymbol{\Phi}_r} = \mathbf{D}^{\mathrm{T}}\boldsymbol{\Phi}_r$ is the effect of the modal shape $\boldsymbol{\Phi}_r$ on the quantity $\mathscr{E}$ and according to equation (4)

$$\gamma_r = \sum_{k=1}^{NS} -\frac{\boldsymbol{\Phi}_r^{\mathrm{T}}\mathbf{M}_{\mathrm{s}}\tilde{\mathbf{R}}_k}{\boldsymbol{\Phi}_r^{\mathrm{T}}\mathbf{M}_{\mathrm{s}}\boldsymbol{\Phi}_r} = -\frac{\boldsymbol{\Phi}_r^{\mathrm{T}}\mathbf{M}_{\mathrm{s}}\mathbf{U}}{\boldsymbol{\Phi}_r^{\mathrm{T}}\mathbf{M}_{\mathrm{s}}\boldsymbol{\Phi}_r} \tag{52}$$

is the commonly used participation factor (i.e. without consideration of spatial variability). With the assumption that peak factors do not vary significantly between ground displacement and ground velocity processes, it follows that

$$\frac{1}{\sigma_u^2}\int_{-\infty}^{+\infty} S_{\ddot{u}}(\omega)\frac{\mathrm{d}\omega}{\omega^2} = \left(\frac{\sigma_{\dot{u}}}{\sigma_u}\right)^2 \approx \left(\frac{\dot{u}_{\max}}{u_{\max}}\right)^2 \tag{53}$$

Also, for lightly damped oscillators, the following approximation holds:

$$\frac{1}{\sigma_r^2}\int_{-\infty}^{+\infty} \omega^2 |h_r(\omega)|^2 S_{\ddot{u}}(\omega)\,\mathrm{d}\omega \approx \frac{\omega_r^2\sigma_r^2}{\sigma_r^2} = \omega_r^2 \tag{54}$$

Equation (49) rewrites

$$\begin{aligned}(E[\mathscr{E}_{\max}])^2 = {} & \mathscr{E}_{\mathrm{U}}^2 u_{\max}^2 + \sum_{r}^{NM} \gamma_r^2 \mathscr{E}_{\boldsymbol{\Phi}_r}^2 D(\omega_r,\zeta_r)^2 + \left(\alpha^2 + \frac{1}{2V^2}\right)\left\{\left(-\sum_{k,l=1}^{NS} a_k a_l d_{kl}^2\right)\dot{u}_{\max}^2\right. \\ & \left. + \sum_{r}^{NM}\left(-\sum_{k,l=1}^{NS} b_k^r b_l^r d_{kl}^2\right)\omega_r^2 D(\omega_r,\zeta_r)^2\right\}\end{aligned} \tag{55}$$

Along the bridge line, define an arbitrary origin O and an orientation. The distance from the origin O to the support point k is measured by the positive or negative number $\bar{d}_{Ok}$. Using the identity $d_{kl}^2 = (\bar{d}_{Ol} - \bar{d}_{Ok})^2$ one obtains equations (10), (11) and (12). It is important to realize that the result is independent of the choice of point O.

APPENDIX II: CURVATURE INDEX

In this section the root mean square of a curvature index for soil displacements is computed in order to show that the expansion of the coherency function does not account for possible soil displacements curvatures. Assume that the apparent wave velocity is infinite (a similar derivation can be carried out for wave passage effects), then the correlation coefficient for displacements at point A and B separated by a distance d is:

$$\rho_{u_A u_B} = \frac{\int_{-\infty}^{\infty} \exp\left[-(\alpha\omega d)^2\right] S_u(\omega)\,\mathrm{d}\omega}{\int_{-\infty}^{\infty} S_u(\omega)\,\mathrm{d}\omega} \tag{56}$$

Using only the first two terms of the Taylor expansion of the exponential function, one has

$$\rho_{u_A u_B} = 1 - (\alpha d)^2 \frac{m_2}{m_0} \tag{57}$$

where m_n is the spectral moment $m_n = \int_{-\infty}^{\infty} \omega^n S_u(\omega)\,d\omega$. Define a curvature index at abscissa x along the bridge line:

$$\delta_2(x) = \frac{u(x+d) - 2u(x) + u(x-d)}{d^2} \tag{58}$$

The limit of $\delta_2(x)$ as d goes to zero is the second derivative of the displacement with respect to x, i.e. the curvature if u is a lateral displacement. The expectancy of the random variable $\delta_2(x)$ is clearly zero and assuming a spatially homogeneous displacement variance σ_u^2, the variance of $\delta_2(x)$ is:

$$E\left[(\delta_2)^2\right] = \frac{\sigma_u^2}{d^4}\left(6 - 4\rho_{u(x+d)u(x)} - 4\rho_{u(x)u(x-d)} + 2\rho_{u(x+d)u(x-d)}\right) \tag{59}$$

Using (57) it is found that $E\left[(\delta_2)^2\right] = 0$, which means that limiting the coherency function expansion to the first two terms implies that the displacements vary linearly along the bridge line in the mean square sense. This approximation and hence the derivation of the approximate formula (10) is only valid for small spatial variations of ground motions.

APPENDIX III: MODAL TRUNCATION ERROR

In this section the modal truncation error for the sum of the square of the base shear forces is examined in the case of partial spatial correlation soil motions. Assuming that the modes are uncorrelated ($\rho_{s_k^r s_l^s} = 0$ for $r \neq s$) but taking into account support motion partial correlations ($\rho_{s_k^r s_l^r} \neq 0$ in general), one obtains:

$$\begin{aligned}\sum_{l=1}^{NS} E\left[|F_l|_{\max}\right]^2 = &\left[\sum_{k,k',l=1}^{NS} \rho_{z_k z_{k'}} \mathbf{K}_{ff,lk} \mathbf{K}_{ff,lk'}\right] z_{\max}^2 \\ &+ \sum_{r=1}^{NM} \sum_{k,k',l=1}^{NS} \rho_{s_k^r s_{k'}^r} (m_r \gamma_{rk} \gamma_{rl})(m_r \gamma_{rk'} \gamma_{rl}) A(\omega_r, \zeta_r)^2\end{aligned} \tag{60}$$

from which the truncation error is found to be:

$$err_{NM'} = \sum_{r=NM'+1}^{NM} \left(\sum_{k,k'=1}^{NS} \gamma_{rk} \gamma_{rk'} \rho_{s_k^r s_{k'}^r}\right)\left(\sum_{l=1}^{NS} \gamma_{rl}^2\right) A(\omega_r, \zeta_r)^2 \tag{61}$$

Now,

$$\left|\sum_{k,k'=1}^{NS} \gamma_{rk} \gamma_{rk'} \rho_{s_k^r s_{k'}^r}\right| \leqslant \sum_{k,k'=1}^{NS} |\gamma_{rk}|\,|\gamma_{rk'}| \tag{62}$$

The right-hand side quadratic form is associated with the $NS \times NS$ symmetrical matrix,

$$\Upsilon = \begin{bmatrix} 1 & 1 & \cdots & 1 \\ 1 & 1 & \cdots & 1 \\ \cdots & \cdots & \cdots & \cdots \\ 1 & 1 & \cdots & 1 \end{bmatrix} = \begin{Bmatrix} 1 \\ 1 \\ \cdots \\ 1 \end{Bmatrix} \begin{bmatrix} 1 & 1 & \cdots & 1 \end{bmatrix} \tag{63}$$

that has only two eigenvalues, namely 0 and NS. It can thus be inferred that the quadratic form is bounded by NS times the Euclidean norm:

$$\sum_{k,k'=1}^{NS} |\gamma_{rk}|\,|\gamma_{rk'}| \leqslant NS \times \sum_{k=1}^{NS} \gamma_{rk}^2 \tag{64}$$

The truncation error is in turn bounded by:

$$err_{NM'} \leqslant \sum_{r=NM'+1}^{NM} NS \times \left(m_r \sum_{l=1}^{NS} \gamma_{rl}^2 \right)^2 A(\omega_r, \zeta_r)^2 \tag{65}$$

or,

$$err_{NM'} \leqslant NS \times \left(\sum_{k=1}^{NS} \tilde{\mathbf{R}}_k^{\mathrm{T}} \mathbf{M}_{\mathrm{s}} \tilde{\mathbf{R}}_k \right)^2 A(\omega_{NM'}, \zeta_{NM'})^2 (1 - r_{\mathrm{TI}}) \tag{66}$$

This shows again that it is relevant to retain enough modes to keep the ratio r_{TI} close to one.

REFERENCES

1. A. Der Kiureghian and A. Neuenhofer, 'Response spectrum method for multiple-support seismic excitation', *Earthquake eng. struct. dyn.*, **21**, 713–740 (1992).
2. N. A. Abrahamson, B. A. Bolt, R. B. Darragh, J. Penzien and Y. B. Tsai, 'The SMART-1 accelerograph array (1980–1987): A review', *Earthquake spectra* **3** (2), 263–287 (1987).
3. R. S. Harichandran and E. Vanmarcke, 'Stochastic variation of earthquake ground motion in space and time', *J. eng. mech.* ASCE **112**, 154–174 (1986).
4. J. E. Luco and H. L. Wong, 'Response of a rigid foundation to a spatially random ground motion', *Earthquake eng. struct. dyn.* **14**, 891–908 (1986).
5. C. H. Loh and Y. T. Yeh, 'Spatial variation and stochastic modeling of seismic differential ground movement', *Earthquake eng. struct. dyn.* **16**, 583–596 (1988).
6. H. Hao, C. S. Oliveira and J. Penzien, 'Multiple-station ground motion processing and simulation based on SMART-1 array data', *Nuclear eng. design* **111**, 293–310, (1989).
7. A. Der Kiureghian, 'A coherency model for spatially varying ground motions', *Earthquake eng. struct. dyn.* **25**, 99–111 (1996).
8. R. S. Harichandran and W. Wang, 'Response of a simple beam to a spatially varying earthquake excitation', *J. eng. mech.* ASCE **114** (9), 1526–1541 (1988).
9. M. Berrah and E. Kausel, 'Spectrum analysis of a beam under non-uniform seismic motion', *Proc. second European conf. on structural dynamics*, Trondheim, Norway, Vol. 1, Balkena, Rotterdam, 1993, pp. 27–32.
10. A. Rutenberg and A. C. Heidebrecht, 'Approximate spectral multiple support seismic analysis: traveling wave approach', *Proc. instn. civil engrs, Part 2*, **85**, 223–236 (1988).
11. Z. Zembaty and S. Krenk, 'Spatial seismic excitation and response spectra', *J. eng. mech.* ASCE **119**, 2449–2459 (1993).
12. H. Hao, 'Arch response to correlated multiple excitations', *Earthquake eng. struct. dyn.* **22**, 389–404 (1993).
13. R. S. Harichandran and W. Wang, ' Response of indeterminate two-span beam to spatially varying seismic excitation', *Earthquake eng. struct. dyn.* **19**, 173–187 (1990).
14. A. Zerva, 'Response of multi-span beams to spatially incoherent seismic ground motions', *Earthquake eng. struct. dyn.* **19**, 819–832 (1990).
15. A. Der Kiureghian and A. Neuenhofer, 'Response spectrum method for incoherent support motions', *Proc. 10th world conf. earthquake eng.* Madrid, 1992.
16. A. Zerva, 'Effect of spatial variability and propagation of seismic ground motions on the response of multiply supported structures', *Probab. eng. mech.* Part 2, **6** (3,4), 212–221 (1991).
17. A. M. Abdel-Ghaffar and L. I. Rubin, 'Suspension bridge response to multiple-support excitations', *J. eng. mech. div.* ASCE **108**, 419–435 (1982).
18. A. M. Abdel-Ghaffar and L. I. Rubin, 'Vertical seismic behavior of suspension bridges', *Earthquake eng. struct. dyn.* **11**, 1–19 (1983).
19. A. M. Abdel-Ghaffar and L. I. Rubin, 'Lateral earthquake response of suspension bridges', *J. struct. eng.* ASCE **109**, 664–675 (1983).
20. A. A. Dumanoglu, J. M. Brownjohn and R. T. Severn, 'Seismic analysis of the Fatih Sultan Mehmet (Second Bosporus) suspension bridge', *Earthquake eng. struct. dyn.*, **21**, 881–906 (1992).
21. A. S. Nazmy and A. M. Abdel-Ghaffar, 'Effect of ground motion spatial variability on the response of cable-stayed bridges', *Earthquake eng. struct. dyn.* **21**, 1–20 (1992).

22. M. Berrah and E. Kausel, 'Modified response spectrum for the design of structures subjected to spatially varying seismic excitations', *Report N. R90-2*, MIT Department of Civil Engineering, Cambridge, Massachusetts, 1990.
23. A. Der Kiureghian and A. Neuenhofer, 'A response spectrum method for multiple-support seismic excitations', *Report N. UCB/EERC-91/08*, University of California at Berkeley, EERC, 1991.
24. M. Berrah and E. Kausel. 'Response spectrum analysis of structures subjected to spatially varying motions', *Earthquake eng. struct. dyn.* **21**, 461–470 (1992).
25. R. W. Clough and J. Penzien, *Dynamics of structures*, McGraw-Hill, 2nd edn, New York, 1993.
26. B. J. Uscinski, *The Elements of Wave Propagation in Random Media*, McGraw-Hill, New York, 1977.